

EXPERIMENTAL AND CFD ANALYSIS OF CO-AXIAL JET

¹G. Ravikumar Solomon, ²Balaji Ramachandran, ³Y. Krishna Vashista Reddy, ³K. Koushik Chandra, ³T. Gokul Nandan, ³M. Srisai

¹Department of Mechanical Engineering, Hindustan Institute of Technology & Science, Tamilnadu, Padur-603103

²NoobTron Private Limited, India

³Department of Aeronautical Engineering, Institute of Aeronautical Engineering, Hyderabad, Telangana 500043

Corresponding Author: sridharabalaa@gmail.com

Abstract:

Jet flows are encountered in many practical applications such as jet engines, gas burners, rockets. To achieve higher spreading rates and to reduce the level of noise, different methods are employed for jet flow control, such as optimizing the shape or using acoustic liners. In this paper, the Circular and non-circular co-axial jets are compared by using flow characteristics. The non-circular shape in this study is hexagonal and cruciform. The circular and non-circular co-axial jets was made and fitted with a blower setup. The flow field characteristics such as the pressure distribution and the velocity distribution of the circular and non-circular co-axial jets were measured using a manometer and pitot tube, respectively. Decay of the jet was investigated at different axial locations quantitatively by measuring pressure in the jet field. The result of the study was validated with the help of CFD analysis using Fluent software. The Reynolds stress mathematical model is used as governing equations for computation. It is observed that non-circular co-axial jets decay at a faster rate, and has low velocity distribution and pressure distribution compared to the circular co-axial jet. It is concluded that circular co-axial jets exhibit optimum flow characteristics compared to the non-circular co-axial jets.

Keywords: Co-axial Jet, momentum coefficient, Reynolds stress model. Velocity distribution, Flow analysis

1. INTRODUCTION

Jets are free shear force driven by the momentum introduced at the exit of a nozzle or an orifice. Jets find a wide range of application in aerospace, commercial industry and domestic life and its use in the modern world with improved technology, various mixing and thrust producing devices [1]. Research in the field of jets in order to gain insight of the flow field has been the focus of study to experimental. several extensive investigations are going on in the field of jets [2].

Extensive work has been carried out on plane and axi-symmetric jets. The jet flow studies have been mostly motivated by two important considerations, namely [3] proper understanding of the jet flow physics controlling the characteristic of the evolving jet. Control of the jet can be either active or passive. Active control of jet requires additional or auxiliary energy source [4]. The most commonly employed active control technique is acoustic forcing. Passive control techniques do not require any additional energy; the control is generally achieved by means of special configurations like notches, tabs and slots, the controlling energy drawn directly from the flow itself, it is used to be controlled. The mixing performances of different nozzles have been compared experimentally [5]. A simple coaxial jet mixer under laminar flow conditions is described. This device demonstrates exceptional control of mixing between two laminar streams by creating shear forces due to variable flow velocities at the points [6]. Jet flows are encountered in many practical applications such as jet engines, gas burners, rockets and others to achieve higher spreading rates, and to reduce the level of noise, different methods are employed for jet flow control [7]. The Structure of Coaxial jet are an integral part of many engineering systems where mixing of streams of different fluid is required. They are used to provide the mixing between fuel and oxidizer in combustors of propulsion systems and power producing gas turbine systems as well as waste combustion and incineration systems [8]. A properly designed jet will efficiently mix the air and fuel while providing the best overall combustion parameters [9]. Single non-circular jets have been shown to have better mixing characteristics than axi-symmetric counterparts [10]. Therefore, combinations of such jets into coaxial configurations are promising. The detailed dynamics of jet entrainment and mixing is of fundamental importance to various applications such as noise suppression, combustion, lift augmentation, heat transfer, and chemical reactors. The present investigation is mainly concentrated on studying the following aspects,

- Flow characteristics of circular and non-circular jets
- Overall centerline pressure decay
- Validation of experimental results with CFD analysis

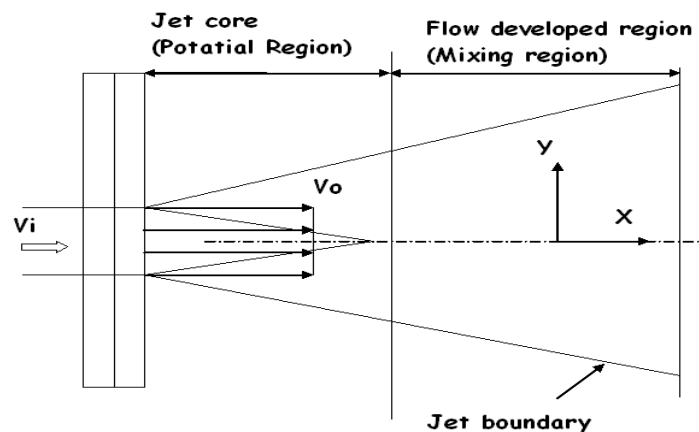


Figure.1 Schematic Diagram of jet structure

2. EXPERIMENTAL METHOD

The geometry chosen for the study is that of a coaxial jet discharging into stagnant laboratory air. Both jets are nominally same pressure. The two stream mixing layer which forms between the center jet and the co flow near the nozzle exit is more compressible. Since this jet is axisymmetric, it requires a minimum number of experimental measurements to fully characterize, and calculations can be performed with relatively modest computer resources. This experiment has been adopted for the CFD development and validation activity.

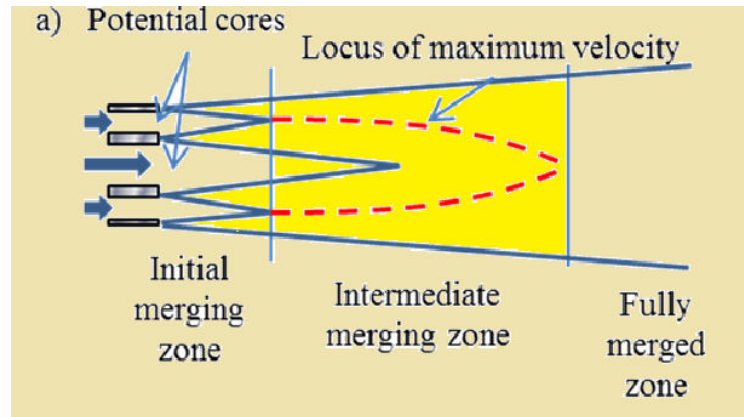


Fig.2 Basic View of Potential Cores of Co-axial Jet

Finite Element Method

Finite element methods use simple piecewise functions (e.g. linear or quadratic) valid on elements to describe the local variations of unknown flow variables. The governing equation is precisely satisfied by the exact solution [11]. If the piecewise approximating functions for are substituted into the equations it will not hold exactly and a residual is defined to measure the errors. Next the residuals are minimized in some sense by multiplying them by a set of weighing functions and integrating. As a result, obtain a set of algebraic equations for the unknown coefficients of the approximating functions.

Fluent

GAMBIT is a software package designed to help analysts and designers build and mesh models for computational fluid dynamics (CFD) and other scientific applications [12]. GAMBIT receives user input by means of its graphical user interface (GUI). The GAMBIT GUI makes the basic steps of building, meshing, and assigning zone types to a model simple and intuitive, yet it is versatile enough to accommodate a wide range of modeling applications.

Finite Volume Method

The finite volume method was originally developed as a special finite difference formulation. The algorithm consists of following steps:

- i. Formal integration of the governing equations of fluid over all the (finite) control volumes of the solution domain.
- ii. Discretisation involves the substitution of a variety of finite difference type approximations for the terms in the integrated equations representing flow processes. This converts the integral equations into a system of algebraic equations [13].
- iii. Solution of the algebraic equations by an interactive method

Spectral Methods

Spectral methods approximate the unknowns by means of Truncated Fourier series. Unlike the finite difference or finite element approach, the approximations are not local but valid throughout the entire computational domain [14, 15]. Again, we replace the unknowns in the governing equations by truncated series. The constraint that leads to the algebraic equations for the coefficient of the Fourier series is provided by a weighted residuals concept similar to the finite element method or by making the approximate function coincide with exact solution at a number of grid points.

3.2 DEVICES USED IN EXPERIMENTAL SETUP

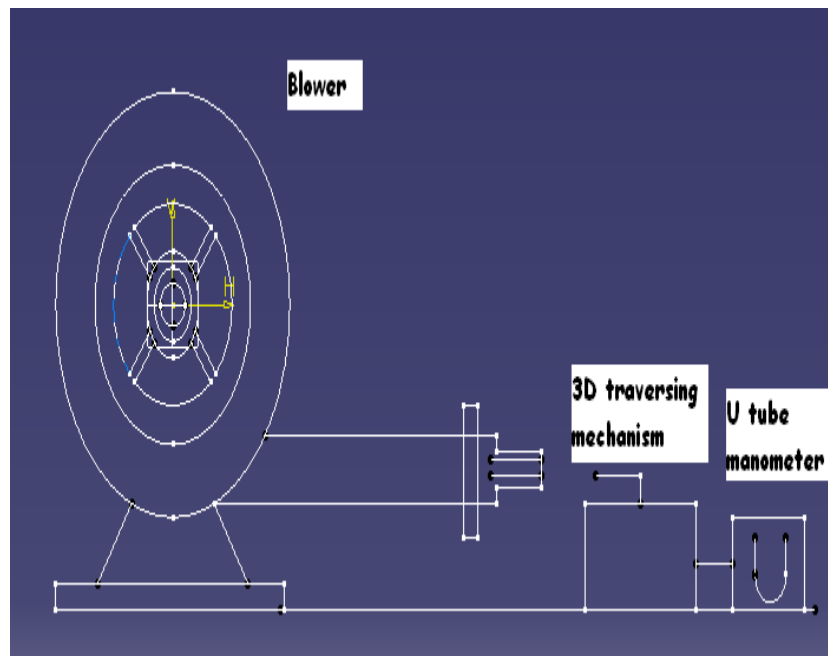


Figure 3.1 Block Diagram of Experimental Setup

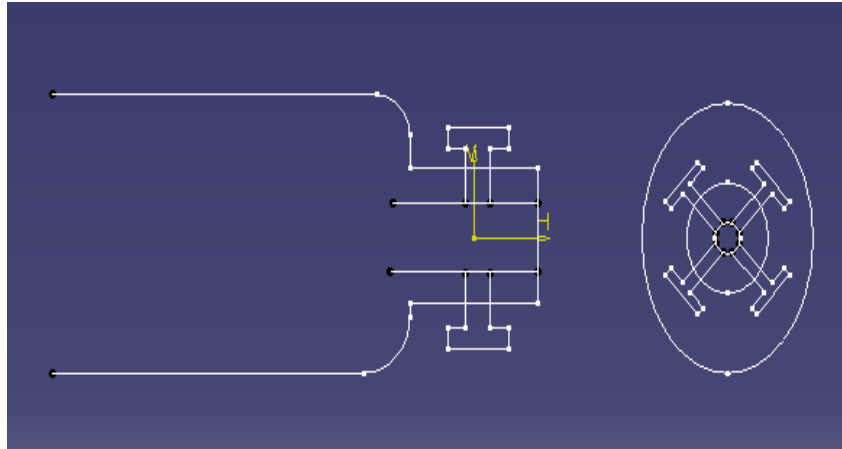


Figure 3.2 Coaxial Jet Setup

3.2.1 Manometer

A manometer is a transparent tube containing a liquid of known density used for the purpose of measurement of fluid pressure. Manometers may be classified as open type manometers useful for measuring the pressure at a point and differential manometers that give the pressure difference between two points of fluid system.

Manometers measure a pressure difference by balancing the weight of a fluid column between the two pressures of interest. Large pressure differences are measured with heavy fluids, Such as mercury (e.g. 760 mm Hg = 1 atmosphere) Small pressure differences are measured by lighter fluids such as water. (27.7 inch H₂O = 1 psi; 1 cm H₂O = 98.1 Pa). A manometer is a device employed to measure pressure. There are a variety of manometer designs. In this project design is a length of glass tubing and then bends the glass tube into a U-shape. The glass tube is then filled with a liquid, typically water. The glass tube is then positioned with the curved region at the bottom. The water settles to the bottom. After the water settles to the bottom of the manometer, the open tubes is connected to the system whose pressure is being measured. In the tubes connected to the system, the gas in the system exerts a force on the water. The net result is that the column of water difference in the tube. The difference in the heights of the columns of water is a measure of the pressure of gas in the system.

The difference in the heights of water in the two columns provides the pressure in units of mm H₂O. (Assume the density of water is 1.00 g.cm⁻³).

Carefully read the heights of the two columns of water in the manometer. Note that the scale is in units of millimeters. Use the two heights to determine the pressure of the system

Equations Used In the Calculation

Pressure(P) is the ratio of the force (F) applied to a surface to the surface area (A).

$$P = F / A$$

So, the pressure p is:

$$P = F / A = mg / A = \rho V g / A = \rho Ah g / A \\ = \rho hg$$

Where g is the acceleration of gravity (9.81 m/s²)

ρ is the density of water is 1.00 g cm⁻³ or 1000 kg /m³)

3.2.2 Pitot Tube

United Sensor stainless steel Pitot – Static probes sense total and static pressures at the same point in a moving fluid. These measurements are often sufficient for calculating flow velocity and weight flow rate if the density is known.

3.2.2.1 Equations used in the calculation

$$V = (2gh)^{1/2}$$

Where V is the velocity at the particular point in m/s

g is the acceleration of gravity (9.81 m/s²).

h is the pressure difference in m

3.3 EXPERIMENTAL SETUP

The coaxial jet assembly is shown in Figure 3.3(a),(b),(c). It is axisymmetric and consists of an outer body and a center body. The passages formed by the space between these bodies, and by the interior passage of the center body, are nozzles designed by the method of characteristic to produce 1 – D flow at their exit.



Figure 3.3 Experimental Setup

3.3.1 3D Sliding Mechanism



Figure 3.4 3D Sliding Mechanism

The 3-Dimensional sliding mechanism is used to measure the pressure in 3 dimensional directions. These were used for moving the Pitot tube in 3D path, and measure he dynamic pressure in all dimensions. The rotating wheel controls each direction.



Figure 3.5(a) Circular Co Axial Jet



Figure 3.5(b) Hexagonal Co Axial Jet

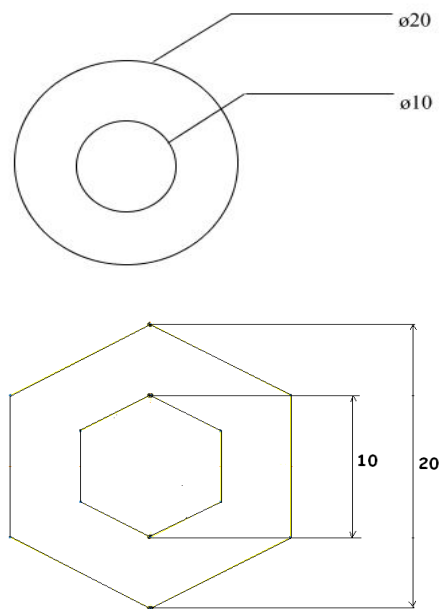


Figure 3.5(c) Cruciform Co Axial Jet

The inner jet has the diameter of 10 mm and the outer jet has the diameter of 20 mm the flow of the two jets was controlled by two valves. Then this jet assembly is to be connected with the reciprocating compressor. This supplies compressed air to the jets.

The 3-Dimensional sliding mechanism is shown in the Figure 3.1. These were used for moving the Pitot tube in 3D path, and measure the dynamic pressure in all dimensions. The rotating wheel controls each direction. Then the Pitot tube is connected with water U-tube manometer so that, able to measure the higher range of pressure differences.

4. JET DIMENSIONS



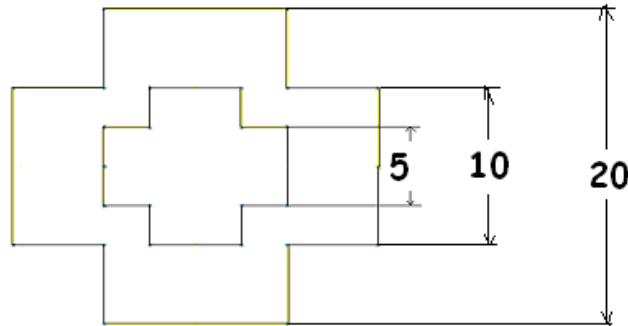


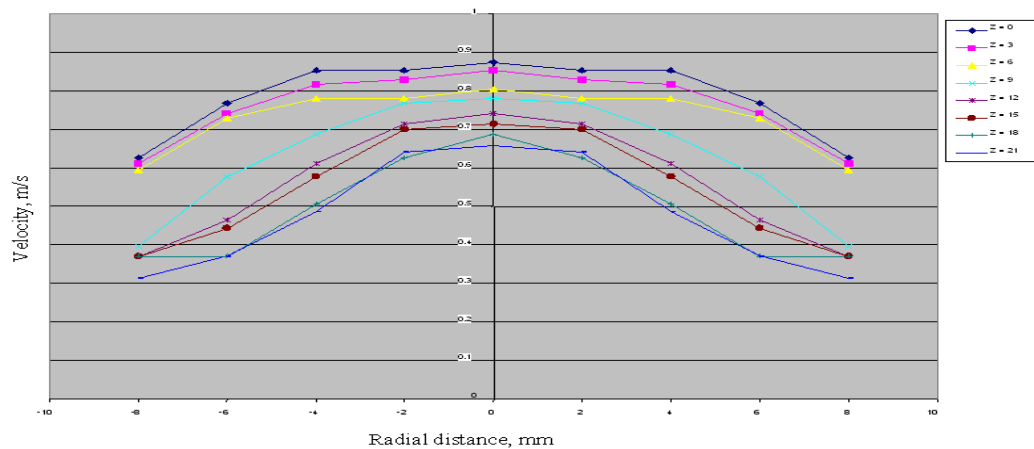
Figure 4. Hexagonal, circular and cruciform jet model dimensions

5. RESULT AND DISCUSSION

The Primary objective of the present investigation is to find the experimental results and it is validate with the CFD analysis using Fluent software by comparing the velocity and pressure for the three cases. We have chosen the hexagonal and cruciform coaxial jets to understand the efficiency of hexagonal and cruciform coaxial jets over circular coaxial jet.

5.1 EXPERIMENTAL RESULTS

Experiments have been carried out in different geometries namely circular, hexagonal and cruciform coaxial jets. The experimental results are compared and presented in the form of profiles at different axial locations for various flow quantities. The experimental velocity and pressure distribution for circular, hexagonal and crucible co-axial jets are compared with radial distance and it is shown in the figures 5.1 to 5.8.



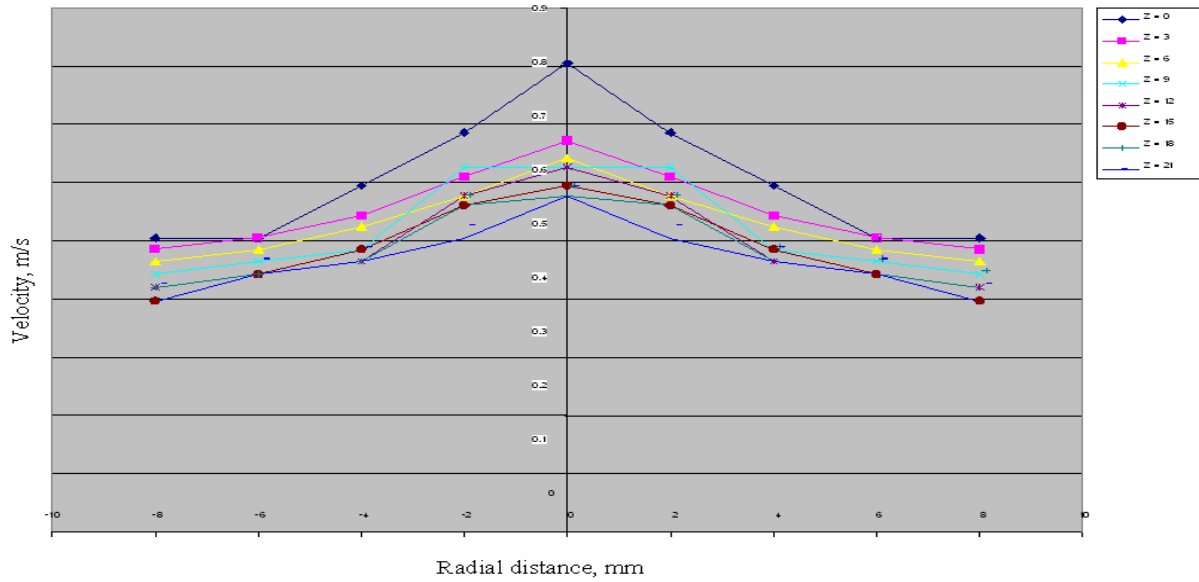


Figure 5.1 Velocity Distribution for Circular Coaxial Jet
Figure 5.2 Velocity Distribution For Hexagonal Coaxial Jet

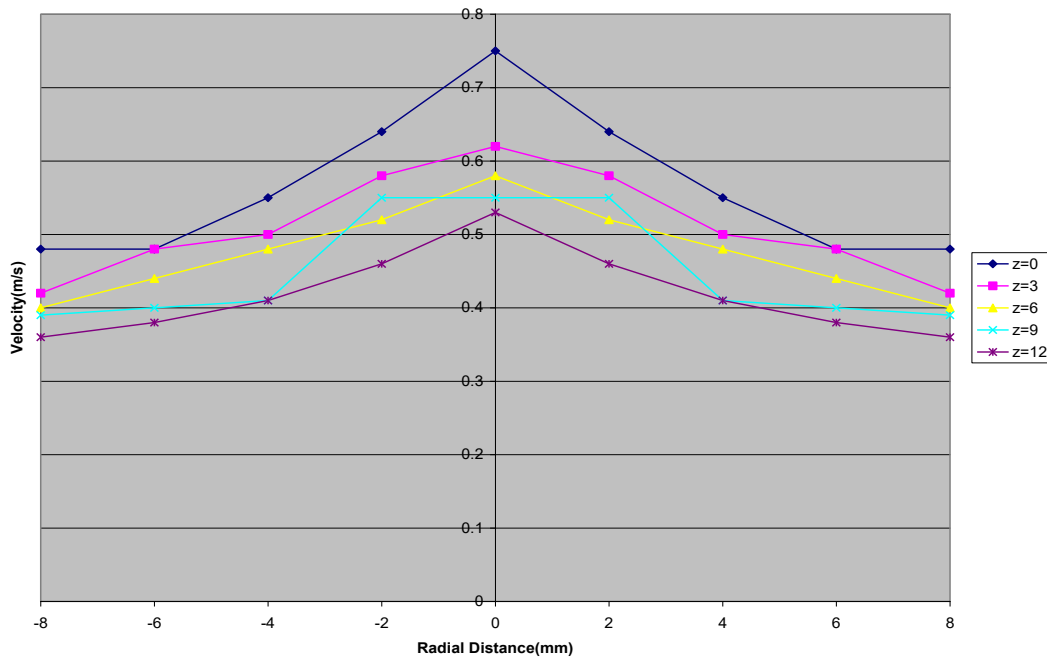


Figure 5.3 Velocity Distribution for Cruciform Coaxial Jet

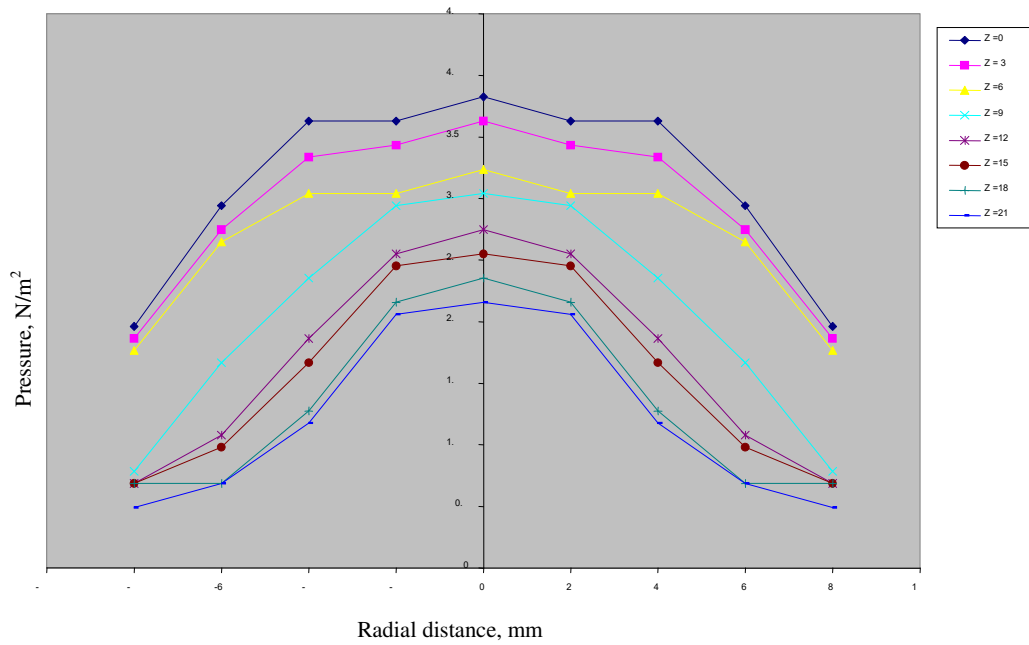


Fig.5.4 Pressure distribution for Circular coaxial jet was plotted between pressure and radial distance

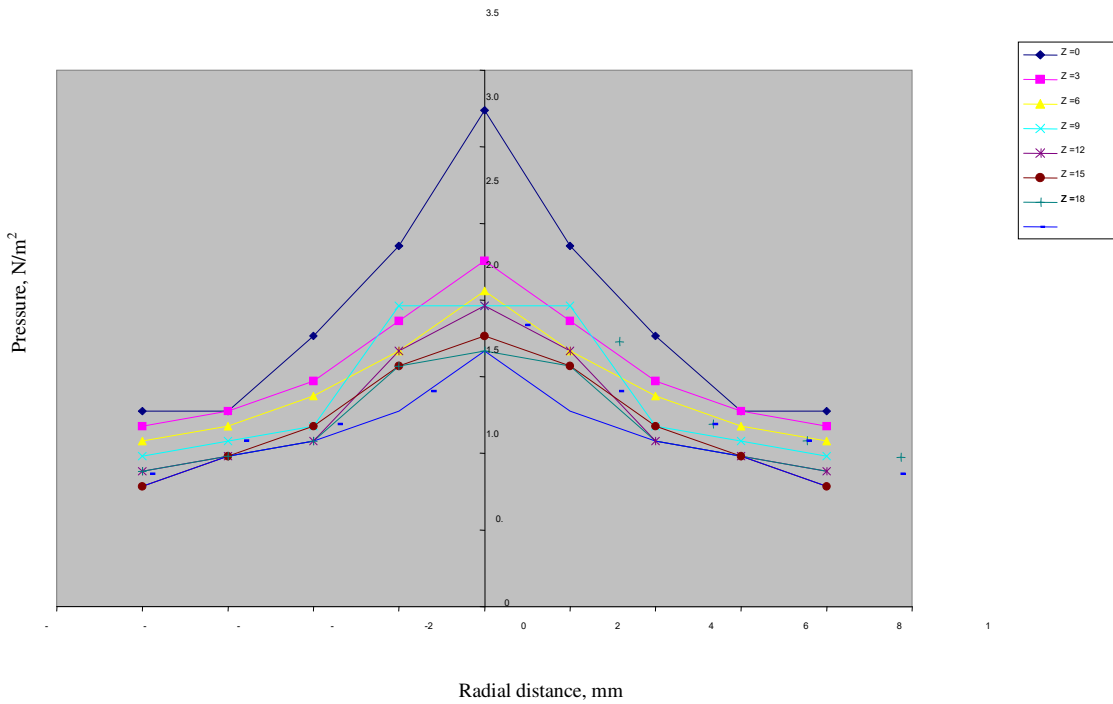


Figure 5.5 Pressure distribution for hexagonal coaxial jet

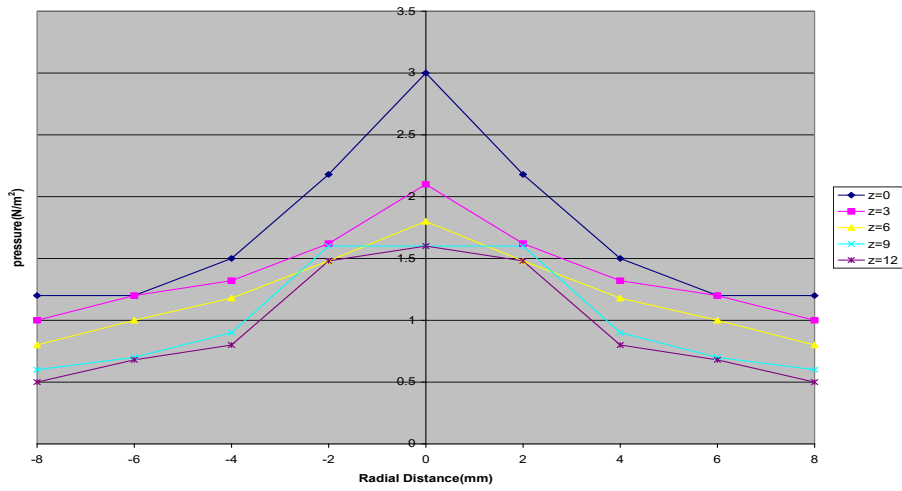


Figure 5.6 Pressure distribution for Cruciform coaxial jet

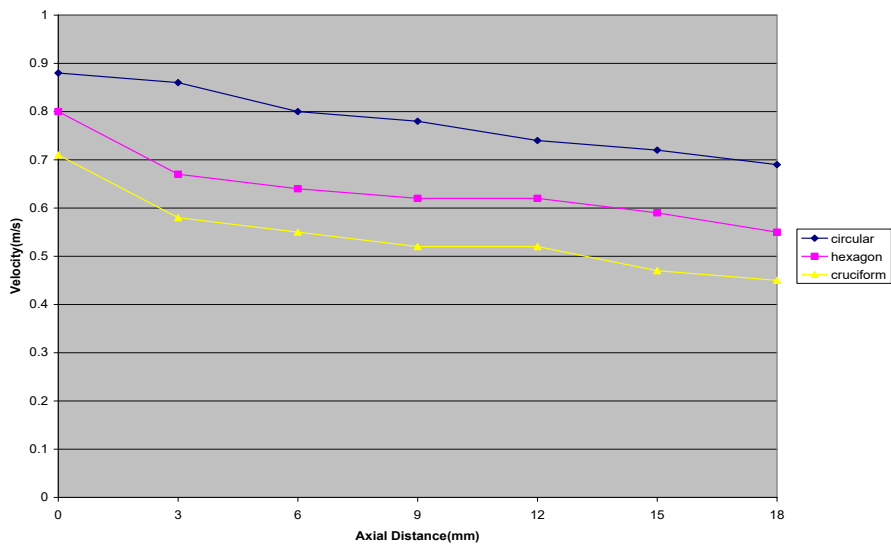


Figure 5.7 Comparison of velocity distribution

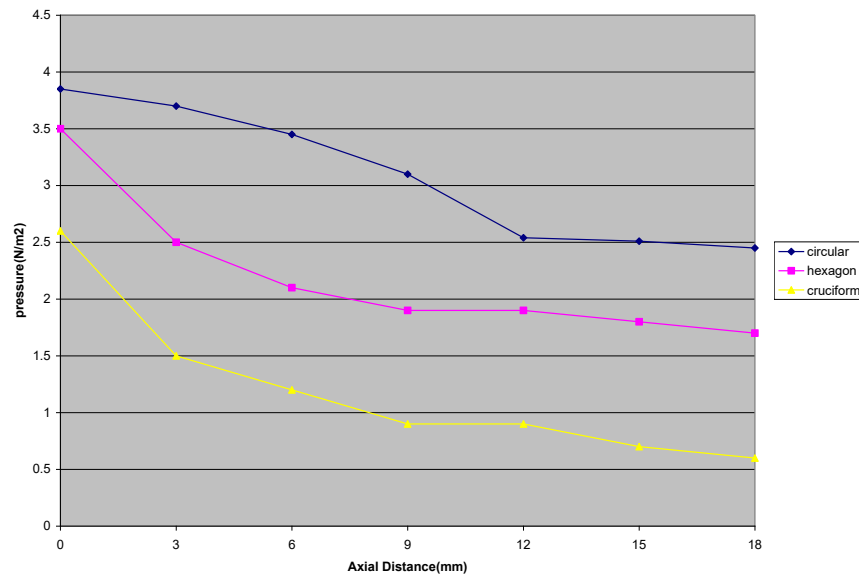


Figure 5.8 Comparison of pressure distribution

From Figure 5.1, Velocity distribution for Circular coaxial jet was plotted between velocity and radial distance. Here in this graph as the axial distance increases the velocity reduces linearly.

From figure 5.2, Velocity distribution for Hexagonal coaxial jet was plotted between velocity and radial distance. Here in this graph as the axial distance increases as the velocity reduces linearly.

From Figure 5.3, Velocity distribution for Cruciform coaxial jet was plotted between velocity and radial distance. Here in this graph as the axial distance increases as the velocity reduces linearly.

From Figure 5.4, Pressure distribution for Circular coaxial jet was plotted between pressure and radial distance. Here in this graph the axial distance increases the pressure reduces linearly.

From Figure 5.5, Pressure distribution for Hexagonal coaxial jet was plotted between pressure and radial distance. Here in this graph the axial distance increases the pressure reduces linearly.

From Figure 5.6, Pressure distribution for Cruciform coaxial jet was plotted between pressure and radial distance. Here in this graph the axial distance increases the pressure reduces linearly.

From Figure 5.7, Comparison of Velocity distribution between circular, hexagonal and cruciform coaxial jet was plotted. Here in this graph the hexagonal and cruciform coaxial jets performance is less than circular coaxial jet.

From Figure 5.8, Comparison of Pressure distribution between circular, hexagonal and cruciform coaxial jet was plotted. Here in this graph the hexagonal and cruciform coaxial jets performance is less than circular coaxial jet.

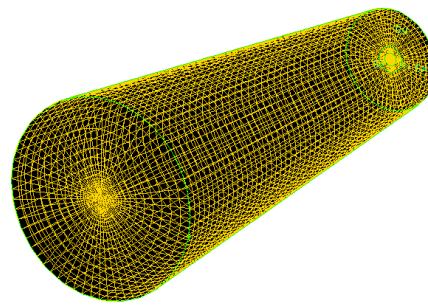
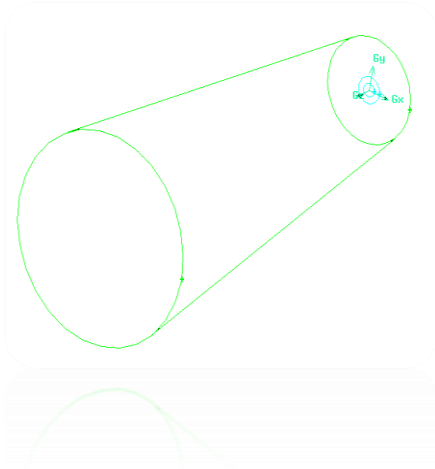


Figure 5.9 Model of the Circular coaxial

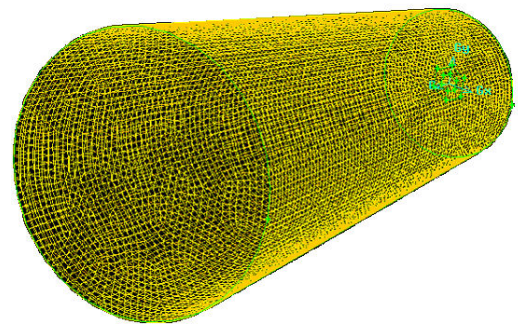
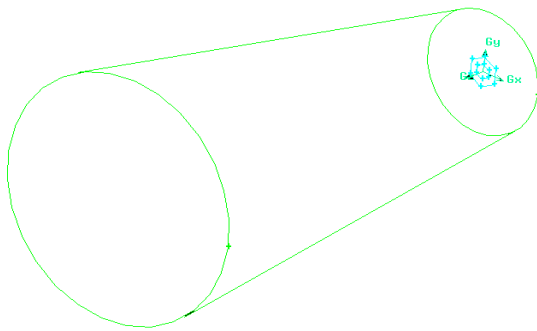


Figure 5.10 Model of the Hexagonal coaxial

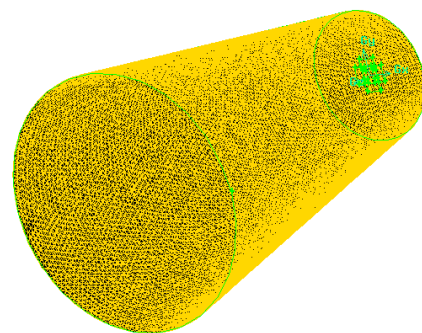
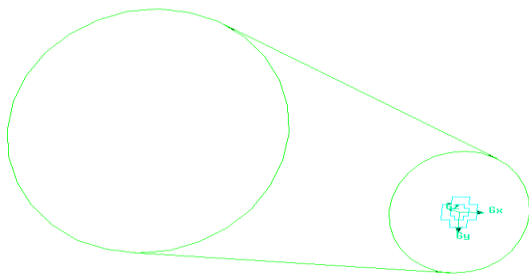


Figure 5.11 Model of the Cruciform coaxial

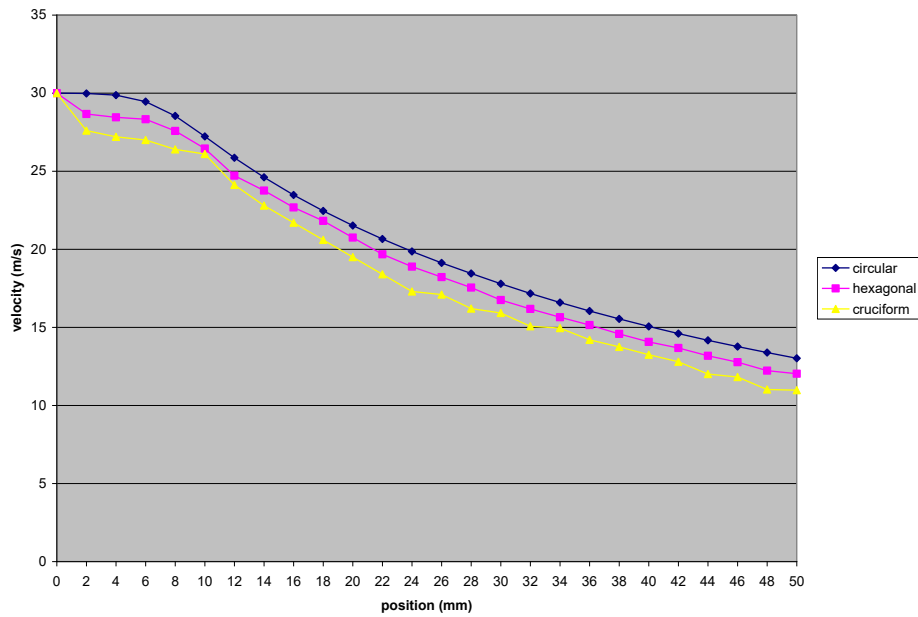


Figure 5.12 Comparison of velocity distribution for axial distance

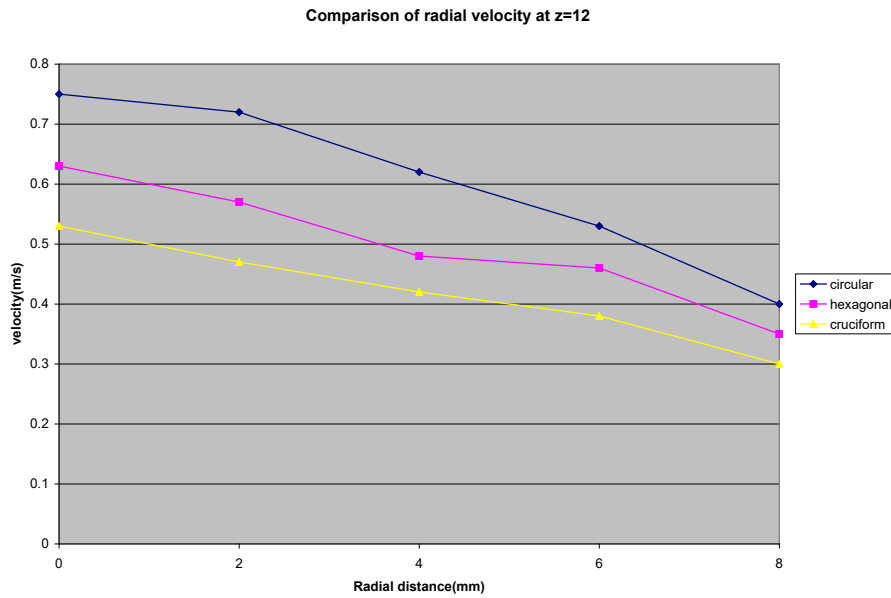


Figure 5.13 Comparison of velocity distribution at Z=12

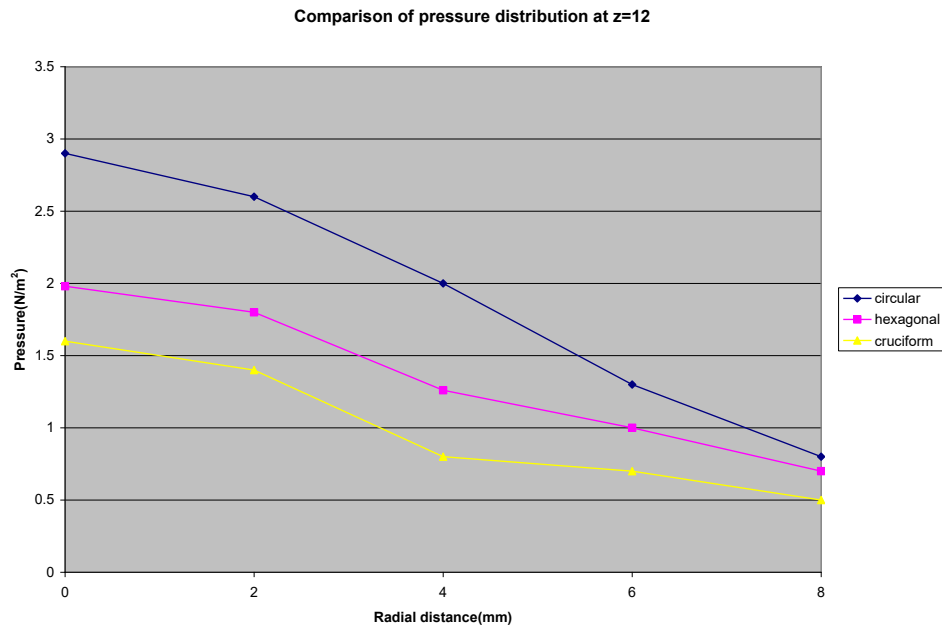


Figure 5.14 Comparison of pressure distribution at Z=12

From Figure 5.13, Comparison of Velocity distribution between circular, hexagonal and cruciform coaxial jet was plotted at a distance Z=12. Here in this graph the hexagonal and cruciform coaxial jets performance is less than circular coaxial jet.

From Figure 5.14, Comparison of Pressure distribution between circular, hexagonal and cruciform coaxial jet was plotted at a distance Z=12. Here in this graph the hexagonal and cruciform coaxial jets performance is less than circular coaxial jet.

CONCLUSION

The experimental and computational analysis for the coaxial jet was done using the experimental setup and CFD software. From the result it is concluded that the non-circular jets (Hexagonal, Cruciform) decay at the faster rate compared to circular jet. The velocity and pressure distribution of non-circular coaxial jet has lower value than the circular coaxial jet. The centerline velocity decay of non-circular jets are faster than the circular jet due to the presence of corner vortices. In this case the cruciform coaxial jet has highest decay and the circular coaxial jet has lowest decay. The result of the decay of the jet was investigated quantitatively at different axial locations and it was validated with the help of CFD analysis using Fluent software. Thus it is found that circular co-axial jet is having higher flow characteristics than hexagonal and cruciform co-axial jet.

Reference:

1. Markesteijn, A.P. and Karabasov, S.A., 2019. Simulations of co-axial jet flows on graphics processing units: the flow and noise analysis. *Philosophical Transactions of the Royal Society A*, 377(2159), p.20190083.
2. Kok, B., Varol, Y., Ayhan, H. and Oztop, H.F., 2017. Experimental and computational analysis of thermal mixing characteristics of a coaxial jet. *Experimental Thermal and Fluid Science*, 82, pp.276-286.
3. Bijarchi, M.A. and Kowsary, F., 2018. Inverse optimization design of an impinging co-axial jet in order to achieve heat flux uniformity over the target object. *Applied Thermal Engineering*, 132, pp.128-139.
4. Panjwani, B., Quinsard, C., Przemysław, D.G. and Furseth, J., 2020. Virtual Modelling and Testing of the Single and Contra-Rotating Co-Axial Propeller. *Drones*, 4(3), p.42.
5. Al-Gailani, A., 2018, Jan. Air flow through an axisymmetric sudden expansion of confined co-axial circular duct: Numerical study. In *2018 (ISCES)* (pp. 146-151). IEEE.
6. Yan, J., Eschricht, D., Thiele, F. and Li, X., 2007. Modeling and Simulation of Coaxial Jet Flow. In *New Trends in Fluid Mechanics Research* (pp. 138-141). Springer, Berlin, Heidelberg.
7. Benham, G.P., Hewitt, I.J., Please, C.P. and Bird, P., 2018. The effect of inner swirl on confined co-axial flow. arXiv preprint arXiv:1805.02961.
8. Seralathan, S., Gupta, J.R., Premkumar, T.M., Balaji, R., Prasanth, D. and Hariram, V., 2019, August. Experimental and Numerical Studies on a Cross Axis Wind Turbine. In *2019 2nd International Conference on Power and Embedded Drive Control (ICPEDC)* (pp. 185-190). IEEE.
9. Suneel, K., Rao, N.N., Balaji, R., Srikanth, N., Solomon, G.R. and Selokar, A., 2020. Review on Sliding Wear of Ti-6Al-4V Alloy Concerning Counterface and Sliding Conditions. In *Intelligent Manufacturing and Energy Sustainability* (pp. 309-318). Springer, Singapore.
10. Balaji, R., Nadarajan, M., Selokar, A., Kumar, S.S. and Sivakumar, S., 2019. Modelling and analysis of disk brake under tribological behaviour of Al-Al₂O₃ ceramic matrix composites/Kevlar® 119 composite/C/Sic-carbon matrix composite/Cr-Ni-Mo-V steel. *Materials Today: Proceedings*, 18, pp.3415-3427.
11. Shankar, R.N., Kumar, K.S., Raja, N.D., Shekar, K.R.C., Raj, N.K. and Gupta, D., 2021. Numerical Study on Supersonic Co-flowing Jet with Varying Lip Thickness. In *Innovative Design, Analysis and Development Practices in Aerospace and Automotive Engineering* (pp. 343-350). Springer, Singapore.
12. Morrall, A., Quayle, S. and Campobasso, M.S., 2020. Turbulence modelling for RANS CFD analyses of multi-nozzle annular jet pump swirling flows. *International Journal of Heat and Fluid Flow*, 85, p.108652.

13. Larsson, I.S., Lycksam, H., Lundström, T.S. and Marjavaara, B.D., 2020. Experimental study of confined coaxial jets in a non-axisymmetric co-flow. *Experiments in Fluids*, 61(12), pp.1-17.
14. Bdeiwi, H. and Ciarella, A., 2021. Computational Fluid Dynamics investigations of a Thrust Reverser Unit flowfield. In *AIAA Scitech 2021 Forum* (p. 0244).
15. Markal, B., Avcı, M. and Aydın, O., 2020. Conical coaxial impinging air jets: angle effect on the heat transfer performance. *Heat and Mass Transfer*, 56(12), pp.3135-3146.